12th IEA Heat Pump Conference 2017

Experimental investigation and dynamic modeling of an air-to-water residential heat pump with vapor injection and variable speed scroll compressor

Bertrand Dechesne[a]*, Samuel Gendebien[a], Vincent Lemort[a], Stéphane Bertagnolio[b]

[a]*University of Liege, Aerospace and Mechanical Engineering Department, Thermodynamics Laboratory, Allée de la Découverte 17, B-4000 Liege, Belgium*
[b]*Emerson Climate Technologies, Aachen, Germany*

Abstract

This paper presents experimental results of a residential air source heat pump using a scroll compressor with variable speed and vapor injection. The system is modeled using the Modelica language and a comparison with the experimental results is performed. It was shown that there is still room for improvement on the control of the system. In fact, the tested gain scheduled PID controller showed limitation to maintain a low and steady superheat on both the suction and injection lines due to dynamics associated to the vapor split line or heat exchangers. The presented model of the system could be used in order to develop model based control and increase the system performances.

Keywords: experimental, air source heat pump, vapor injection, scroll compressor, Modelica, dynamic modeling

1. Introduction

Ever-increasing power of computational packages and processors allows engineers to develop more advanced control strategies, the field of vapor compression system is no exception to the rule. Dynamic modeling helps to develop and test these new control strategies in order to increase the system performances. In this field, Rasmussen et al. provides a deep literature review and a complete simulation tutorial for the dynamic modeling of vapor compression cycles ([1] and [2]). Hongtao et al. ([3] and [4]) studied a flash tank injection heat pump and developed a model in Modelica language. However, the studied compressor is a fixed speed scroll compressor. In [4], the authors presented the validation of their dynamic models for both system start-up and shut-down procedures. Jiazhen et al. [5] evaluated the steady-state and transient behavior of a heat pump working with different low-GWP refrigerants (R32 and D2Y60). In 2011, Li et al. [6] developed a dynamic model of a R134a automotive air-conditioning and showed the refrigerant mass migration during start-up and shut-down operations.

This paper presents experimental results and a Modelica-based dynamic model of an air source heat pump (ASHP) using a variable speed vapor injection scroll compressor and R410A as working fluid. This model is based on the open-source and open-access ThermoCycle library [7] for the model components and CoolProp for the fluid thermodynamic properties [8]. An empirical model of the vapor injection scroll compressor is developed using

* Corresponding author. Tel.: +32 4 366 48 00; fax: +32 4 366 48 12.
E-mail address: bdechesne@ulg.ac.be.

empirical correlations for the volumetric efficiency, isentropic efficiency and the ratio between the injection and suction mass flow rates. PID controllers are used to control the needle position of the electronic expansion valve in order to obtain a target superheat on the injection line and at the exhaust of the evaporator.

Table 1. List of subscripts

Subscripts			
su	Suction port	cd	Condenser
ex	Exhaust port	ev	Evaporator
inj	Injection port	g	Growth
r	Refrigerant	d	Densification
v	Volumetric	ieev	Injection electronic expansion valve
s	Isentropic	oeev	Outdoor electronic expansion valve
cp	Compressor		
eco	Economizer		

2. Experimental investigation

2.1. System overview

The studied system is a residential air-to-water heat pump. The compressor is variable speed and uses vapor injection in order to achieve higher pressure ratios and condensing pressures. The system is an internal heat exchanger (i.e. economizer) injection cycle type and is composed of two separated units (indoor and outdoor). The outdoor unit is composed of the evaporator and the main electronic expansion valve. Between these two units, split lines are present, one of these is the vapor line, between the evaporator and the compressor suction. The other one is the liquid split line and is located between the exhaust of the drive cooler and the inlet of the outdoor electronic expansion valve. These split lines can reach up to 20 meters and have a major impact on the system dynamics. The drive cooler is a small heat exchanger made up of an aluminium plate in contact with both refrigerant tubes and the drive electronic circuit in order to cool down the latter.

2.2. Test bench description

The present section aims at describing the apparatus developed to carry out experimental investigations on the air-to-water heat pump. A schematic representation of the test bench is given in Fig. 1. The blue and red refrigerant lines are respectively only used in cooling or heating mode. However, in the rest of the paper, the reversible heat pump is supposed to work only in heating mode.

2.2.1. Outdoor room

The outdoor unit is installed in a room where conditions are controlled in terms of both humidity and temperature. Relative humidity is controlled by the use of electrical steam generators (humidifier). It is also possible to control with precision the outdoor air temperature by means of a set of variable electrical resistances. Outdoor unit conditions are controlled by means of a PID integrated in the Labview controller. An air mixing fan is used to ensure conditions homogeneity all over the outdoor room. The relative humidities at the inlet and at the outlet of the outdoor air stream passing through the air evaporator are measured by means of relative humidity sensors with an accuracy of ± 1.5 percent points.

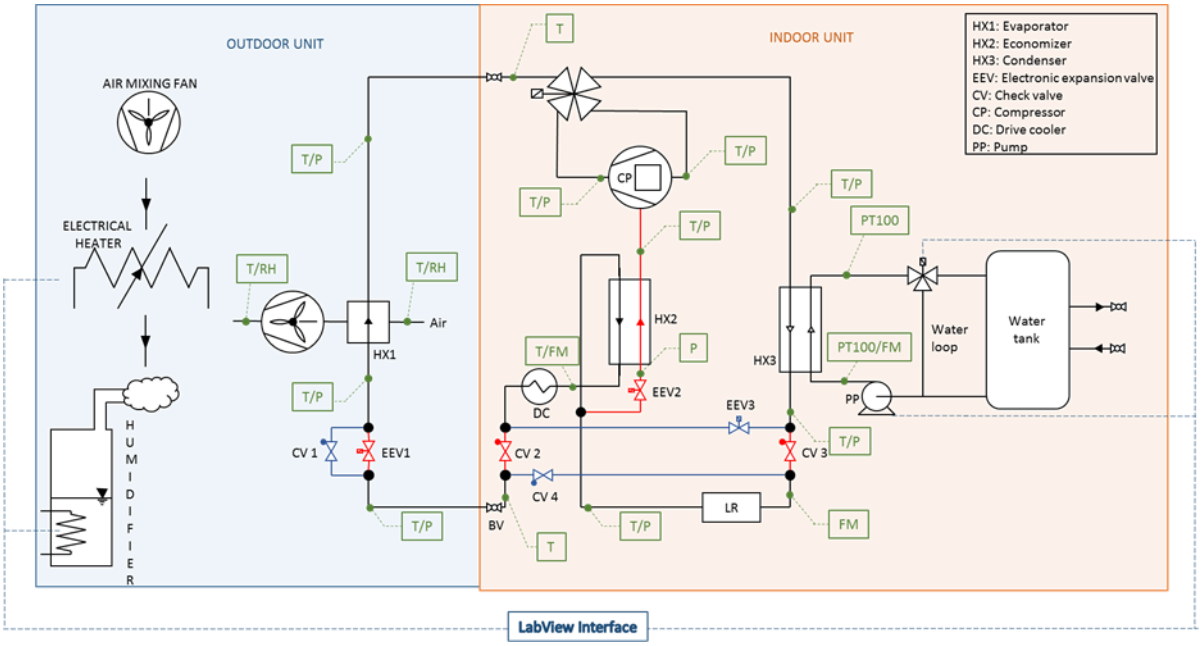

Figure 1: Schematic representation of the test bench

2.2.2. Refrigerant loop

The refrigerant loop is controlled by means of a ModBus Interface, which implies the adjustment of the rotational speed of the air evaporator fan, of the scroll compressor, the openings of the expansion valves as well as the four-ways valves. The drive cooler is an additional heat exchanger installed to cool down the power electronic used for the variation of the compressor speed.

Conditions in terms of temperature and absolute pressure are measured at the supply/exhaust of each component of the refrigerant loop. Temperatures are determined by means of sensor pocket (type T thermocouple) with accuracy of ±0.3 K. Used absolute pressure sensors show the following characteristics:

- Operating range of 0-20 bar for the sensor used at the supply of the compressor with an accuracy of 1% of the full scale range,
- Operating range of 0-30 bar for sensors used for measuring the low and intermediate pressure level with an accuracy of ±1% of the full scale range,
- Operating range of 0-50 bar for sensors used for measuring the high pressure with an accuracy of ±0.5% of the full scale range.

The refrigerant flow rate at the exhaust of the condenser is measured by means of a Coriolis flow meter with an absolute error varying between 0.3 and 1.5g/s (depending on the measured flow rate). Error related to the use of flow meter used for the determination of the refrigerant flow rate passing through the high pressure side economizer varies between 0.33 and 1.7 g/s (also depending on the measured flow rate).

2.2.3. Water loop

Water flow rate passing through the condenser is controlled by adjusting the rotational speed of the water

pump. The water temperature at the supply of the condenser is adjusted by a PID controlling the opening of a three-ways valve. This latter is supposed to mix a flow rate coming from the exhaust of the condenser and another one coming from the water tank. This latter is used as a heat sink that can be either cooled continuously by means of tap water or heated up via variable electrical resistances. Given the low temperature difference between the supply and the exhaust of the condenser (between 3 and 10K), PT100 with accuracy of ±0.1 K have been preferred instead of type T thermocouple. Water flow rate is determined by means of an impulse water meter (4 pulses per liter).

Table 2. List of sensors

Sensors	Error
Type T thermocouples	±0.3 K
PT100 class 1/10 DIN	±0.1 K
Keller 0-20 bar absolute pressure	±0.2 bar
Keller 0-30 bar absolute pressure	±0.3 bar
Keller 0-50 bar absolute pressure	±0.25 bar
Krohne Optimass 6000	±0.33 to 1.7g/s
Emerson micro-motion CMF025	±0.3 to 1.5g/s
Impulse water meter	4 pulses per liter

3. Experimental results

This section aims at presenting the experimental results as well as highlighting the possible improvements of the heat pump. The advantages of the variable speed and the injection are also presented. The heat pump was tested in a wide variety of working conditions presented in Tab. 3. The condensing and evaporating temperature are defined for a quality of 1 and respectively the pressure at the condenser inlet and at the evaporator exhaust.

Table 3. Testing conditions ranges

Variables	Min. Value	Max Value
Compressor speed [rpm]	3000	7000
Water inlet temperature [°C]	30.6	56.2
Water temperature increase [K]	4.3	9.5
Outside air temperature [°C]	-3	35
Condensing temperature [°C]	38	62
Heating capacity [W]	6200	12100
Evaporating temperature [°C]	-15.4	16.8

3.1. Partial load results

Having a variable speed compressor allows the heating capacity to be varied by controlling the compressor speed and is supposed to maintain system performance at partial load. Fig. 2 shows the variation of the second law coefficient of performance (COP_{II}) of the heat pump as a function of the rotational speed of the compressor. The COP_{II} is the ratio of the actual COP of the system to the Carnot COP defined in the same working conditions as the studied system. The heat source and heat sink temperatures for the calculation of the Carnot COP were chosen to be the condensing and evaporating temperatures of the system as defined in the previous section.

It can be conclude that for a rotational speed varying between 3500 and 7000 rpm, the performance of the system is not significantly impacted.

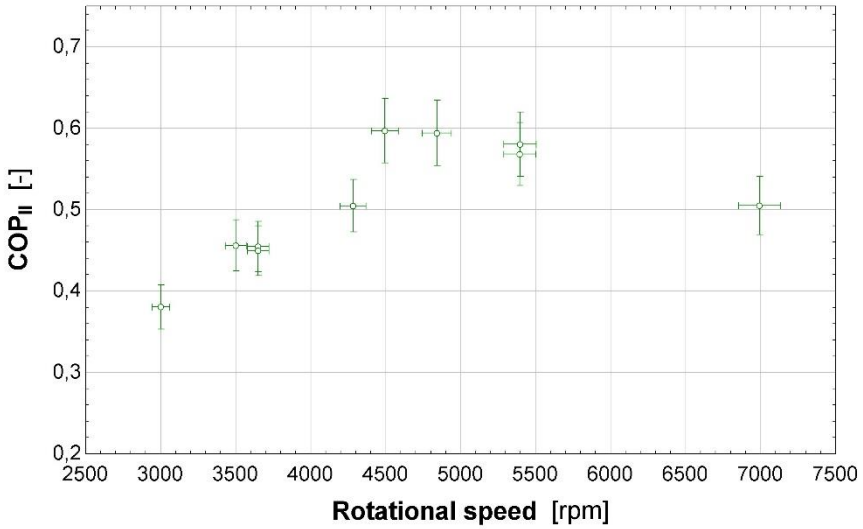

Figure 2: Second law COP vs compressor rotational speed

3.2. Winter conditions

The main advantage of the injection is to lower the discharge temperature and thus allow the compressor to work with higher pressure ratio. The system should then be able to produce high temperature domestic hot water even under winter conditions. The heat pump was tested under an outside temperature of -3°C and a supply water temperature of 55°C at the condenser inlet. The system performances for a maximum rotational speed of 7000 rpm are given in Tab. 4.

Table 4. Winter conditions performances

Variables	Value
Compressor speed [rpm]	7000 ± 140
COP [-]	2.28 ± 0.15
Compressor discharge temperature [°C]	127.7 ± 0.1
Water inlet temperature [°C]	55.0 ± 0.1
Water outlet temperature [°C]	59.4 ± 0.3
Outside air temperature [°C]	-3 ± 0.3
Heating capacity [W]	8265 ± 364

The system is thus capable of providing a heating capacity of more than 8 kW by heating water to about 60°C with a COP of 2.28 and for an outside temperature of -3°C.

3.3. Superheat control

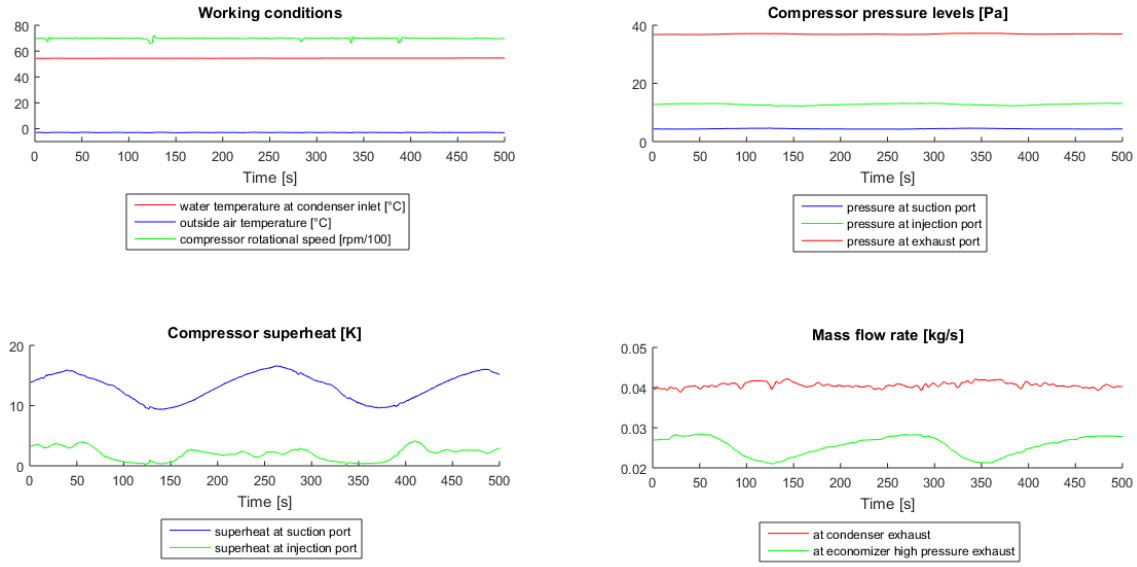

Figure 3: Superheat control for steady operating conditions

Figure 3 shows experimental results where the control of the superheat can be observed. The first graph shows that the working conditions of the system are fixed as the rotational speed, the water inlet temperature and the outside air temperature are almost constant. However, it can be seen that the control of both superheats, on the suction and injection lines, is not optimum as the superheats are not stabilized. This is due to the fact that the current control uses a decoupled adaptive PID controller with no feed-forward action. The control of the superheat, especially on the suction line is made difficult by the presence of the suction line which has a significant impact on the response of the superheat at the suction of the compressor for a given variation of the valve opening.

It can be concluded that, because of the complexity of the system, the current controller could be improved. In this context, a dynamic model of the heat pump was developed in order to design more advanced control strategies.

4. Modeling

This section presents the dynamic model of the heat pump, developed in the Modelica language. The main components of the systems are described.

4.1. Compressor

The proposed model uses a set of five dimensionless polynomials to predict the compressor behavior. The compressor model is treated as quasi steady-state, in fact, the time constants associated to the compressor dynamics are very small compared to those associated with heat exchangers and charge distribution [5]. The inputs of the compressor polynomials are the rotational speed rpm and the three pressure levels, i.e. the suction pressure P_{su}, injection pressure P_{inj} and discharge pressure P_{ex} or combinations of these pressures, i.e.

$$r_{p,tot} = \frac{P_{ex}}{P_{su}} \quad \textit{, the total pressure ratio} \tag{1}$$

$$r_{p,inj} = \frac{P_{inj}}{P_{su}} \quad \textit{, the injection pressure ratio} \tag{2}$$

The mass flow rates, exhaust state and compressor consumption can be computed thanks to the five

polynomials which are the volumetric and isentropic efficiencies (η_v and η_s), the drive efficiency (η_{drive}), the injection ratio (X_{inj}) and the losses ratio (X_{loss}). Finally, the model can be written as follows:

$$\dot{M}_{r,su} = \varepsilon_v\left(rpm, P_{su}, P_{inj}, P_{ex}\right) . \rho_{r,su} . V_s . N_{rot} \tag{3}$$

$$\dot{M}_{r,inj} = X_{inj}\left(rpm, P_{su}, P_{inj}, P_{ex}\right) . \dot{M}_{r,su} \tag{4}$$

$$\dot{W}_{in} = \frac{\dot{W}_s}{\varepsilon_s\left(rpm, P_{su}, P_{inj}, P_{ex}\right)} \tag{5}$$

$$\dot{W}_s = \dot{M}_{r,su} . \left(h_{r,ex,s} - h_{r,su}\right) + \dot{M}_{r,inj} . \left(h_{r,ex,inj,s} - h_{r,inj}\right) \tag{6}$$

$$\dot{W}_{el} = \frac{\dot{W}_{in}}{\eta_{drive}\left(rpm, P_{su}, P_{inj}, P_{ex}\right)} \tag{7}$$

$$\dot{Q}_{loss} = \dot{W}_{el} . X_{loss}\left(rpm, P_{su}, P_{inj}, P_{ex}\right) \tag{8}$$

Where $\dot{W}_{in}$ is the electrical power delivered to the compressor motor and $\dot{W}_s$ the isentropic power. This latter is composed of two terms related to the isentropic compression of two separate volumes performing the compression process from the suction to the discharge pressure for the first one and from the injection to the discharge pressure for the second one. This model has been calibrated with manufacturer data and proved to predict the performance, mass flow rates and exhaust state accurately for two different scroll compressors as presented in more details in [10].

4.2. Heat exchangers and split lines

Heat exchanger models are based on the finite volume method where the energy and mass conservation equations are applied to several cells connected in series, more information can be found in [7]. The dynamics taken into account in this model comes from the metal wall and the volume of fluid enclosed in the heat exchanger.

The fluid cells are thus connected to a metal wall with which heat is exchanged. However, no longitudinal conduction is taken into account. The main parameters of the dynamic heat exchangers models are the number of cells on each side, geometrical features such as the heat transfer area and the heat transfer coefficients (HTC) between both fluids and the metal wall. Different options are implemented to take into account the variation of the HTC (see [7]), in this case, a constant HTC in each zone (subcooled – two phase - superheated) was chosen. In fact, it was shown in [10] that, due to the low pinch point values, the heat transfer coefficient variations do not affect greatly the predicted heat transfer rate. This heat exchanger model is used for the condenser and economizer. About the drive cooler heat exchanger, due to its small size, no dynamics is assumed and the drive losses are directly injected into the refrigerant stream.

The split lines model is based on the same fluid cells, which are also connected in series and to a metal wall representing the split line tube. These split lines are however buried in the ground in residential applications and are thus assumed to be adiabatic.

The evaporator model takes into account the moist air condensation using the Lewis analogy. Similarly to the condenser and economizer models, the refrigerant flow is divided into *n* fluid cells connected in series. In order to model the cross-flow heat exchanger, the air flow rate is divided into *n* cells in parallel. In this configuration, each air cell exchanges heat with one of the refrigerant cell. The temperature difference between the inlet and outlet of a refrigerant cell is quite small as the cells on the refrigerant side are in series, however, this remark is not correct

on the air side as the cells are in parallel. The sensible heat exchange rate is thus computed using the $\varepsilon - NTU$ method and the latent heat exchange rate is determined via the Lewis analogy.

The structure of the Modelica model is shown in Fig. 4. Fig.4 *(a)* presents the model of the refrigerant fluid flow which is connected to a thermal inertia represented as a metal wall. This wall is connected on the other end to the air cells connected in parallel. Fig.4 *(b)* shows the air side model with *n* cells in parallel. The linear pressure drop on the air side is directly implemented in the cell as a function of the air mass flow rate.

A frost model is implemented in the moist air cell. This model is based on the work of Hermes et al. [14] and Lee et al. [9]. Most of the models in the literature are based on a series of assumptions:

- All processes (mass and heat transfer) are treated as a quasi-steady state and one dimensional phenomenon;
- The frost density is a layer-averaged value at any moment;
- The air pressure is uniform in the air stream and within the frost layer;
- The thermal conductivity of frost is a function of density;
- The frost thickness was assumed uniform along the wall;
- The Lewis analogy (analogy between heat and mass transfer) is applicable

Most of the models consist in dividing the overall mass flux into two parts, called the growth $\dot{m}_g$ (contributing to increase the frost layer thickness) and the densification $\dot{m}_d$ (contributing to increase the frost layer density) mass fluxes.

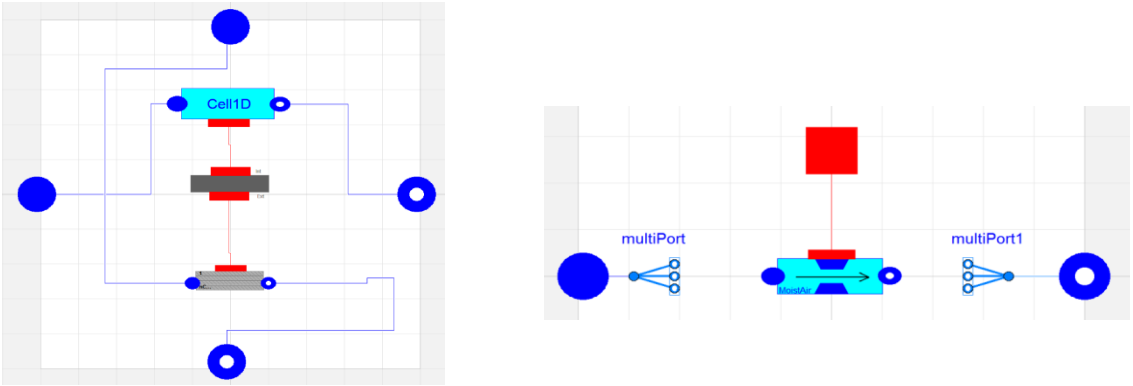

(a) (b)

Figure 4: Evaporator Modelica model structure

4.3. Expansion devices

The expansion valve is an important component of vapor compression systems. In fact, the control of the superheat is possible by varying the valve opening.

Several electronic expansion valve (EEV) models are available in the literature. Bach et al. [18] developed a dimensionless law for the valve mass flow using the Buckingham PI-theorem. This law is valid for two-phase inlet conditions and for two refrigerants (R410a and R404a). Park et al. [20] also presented empirical laws for an EEV working with either R22 or R410a. The correlation yielded satisfactory predictions within a relative deviation of 15.0%. In the frame of this work, a new correlation for the coefficient of correction C_d was developed thanks to the experimental campaign results. The mass flow rate passing through the valve is calculated as follows:

$$\dot{m}_{EEV} = C_d \,.\, A_{full} \,.\, \sqrt{2 \,.\, \rho_{su,EEV} \,.\, \Delta P_{EEV}} \tag{9}$$

Where

- A_{full} is the valve full opening and was measured, for both the main and injection expansion valve, on a laser cut expansion valve (see Fig. 5);
- $\rho_{su,EEV}$ is the density at the valve suction;
- ΔP_{EEV} is the pressure difference between the inlet and outlet of the valve.

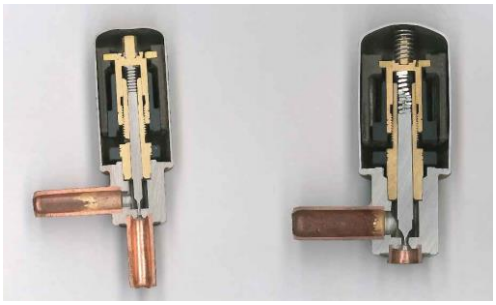

Figure 5: Cut expansion valves

As stated here above, the electronic expansion valves (EEV) have been studied by numerous authors. However, the correlations developed by Bach [11] and Park [12] were not adapted for the system studied in this paper. New correlations were developed for the discharge coefficient C_d of both the injection and outdoor EEVs thanks to experimental data. The goal is to develop a simple model of the valve for control and not develop a general one that is valid for different types of valve or fluid. The mass flow is calculated via Eq.9 with a coefficient of determination given by the following equation:

$$C_d = a_0 . \pi_1^{a_1} . \pi_2^{a_2} \quad (10)$$

Where π_1 and π_2 are two dimensionless groups respectively equal to the inlet pressure over the critical pressure and the effective area over the full opening area of the valve. The parameters are given in Tab.5, the mass flow is determined with a maximum error of 8% and a standard deviation of respectively 4.2 and 5.5% for the outdoor and injection expansion valves.

Table 5. Expansion valves parameters

Parameters	IEEV	OEEV
A_{full} [m²]	1.227E-6	4.524E-6
a_0 [m^{-1}]	0.3048	0.4029
a_1 [-]	-0.3834	-0.3834
a_2 [-]	0.493	1.022

4.4. Liquid receiver

This tank is placed at the exhaust of the condenser and is filled with saturated liquid and vapor. The liquid receiver is considered as one control volume and modeled using the energy and mass conservation principles assuming thermodynamic equilibrium at all times inside the control volume. The refrigerant charge is imposed by the initial conditions in the heat exchangers, split lines and tank. Hence, by varying the initial level in the liquid receiver, it is possible to adjust the total refrigerant charge in the cycle without changing the working conditions

5. Conclusions and future work

The experimental investigation showed that the studied system is able to provide domestic hot water even for severe winter conditions. It was shown that the performance at partial load is not decreasing significantly thanks to the variable speed compressor.

Moreover, the control of the superheat, both for the injection and suction line could be improved. This is due to the complex dynamics associated with the vapor split line, the evaporator and the economizer. Furthermore, these systems are coupled and interact with each other.

This last observation yield to the conclusion that a dynamic model was needed in order to develop more advanced control. Based on Park [12], two sets of parameters were determined for the injection and outdoor electronic injection valve in order to predict the mass flow rate with a maximum error of 8%. The developed dynamic model will help, after validation, to develop new control strategies (e.g. model base or model predictive control) and improve the decoupled adaptive PID controller that was tested in this study.

Acknowledgements

The authors would like to acknowledge Emerson Climate Technologies who sponsored a part of the test bench.

References

[1] Rasmussen, Bryan P. "Dynamic modeling for vapor compression systems - Part I: Literature review." HVAC&R Research 18, no. 5 (2012): 934-955.
[2] Rasmussen, Bryan P., and Bhaskar Shenoy. "Dynamic modeling for vapor compression systems - Part II: Simulation tutorial." HVAC& R Research 18.5 (2012): 956-973.
[3] Qiao, Hongtao, Xing Xu, Vikrant Aute, and Reinhard Radermacher. "Transient modeling of a flash tank vapor injection heat pump system - Part I: model development." International Journal of Refrigeration 49 (2015): 183-194.
[4] Qiao, Hongtao, Xing Xu, Vikrant Aute, and Reinhard Radermacher. "Transient modeling of a ash tank vapor injection heat pump systemPart II: Simulation results and experimental validation." International Journal of Refrigeration 49 (2015): 183-194.
[5] Ling, Jiazhen; Qiao, Hongtao; Alabdulkarem, Abdullah; Aute, Vikrant; and Radermacher, Reinhard, "Modelica-based Heat Pump Model for Transient and Steady-State Simulation Using Low-GWP Refrigerants" (2014). International Refrigeration and Air Conditioning Conference. Paper 1421. http://docs.lib.purdue.edu/iracc/1421
[6] Li, Bin, Ste_en Peuker, Predrag S. Hrnjak, and Andrew G. Alleyne. "Refrigerant mass migration modeling and simulation for air conditioning systems." Applied Thermal Engineering 31, no. 10 (2011): 1770-1779.
[7] Quoilin, Sylvain; Desideri, Adriano; Wronski, Jorrit; Bell, Ian; and Lemort, Vincent, "ThermoCycle: Modelica library for the simulation of thermodynamic systems" (2014). Proceedings - 10th International Modelica Conference; doi:10.3384/ECP14096683
[8] Bell, Ian H., JorritWronski, Sylvain Quoilin, and Vincent Lemort. "Pure and pseudo-pure fluid thermophysical property evaluation and the open-source thermophysical property library Coolprop." Industrial & engineering chemistry research 53, no. 6 (2014): 2498-2508.
[9] Kwan-Soo Lee, Woo-Seung Kim, and Tae-Hee Lee. A one-dimensional model for frost formation on a cold at surface. International Journal of Heat and Mass Transfer, 40(18):4359{4365, 1997.
[10] Dechesne, Bertrand; Bertagnolio Stéphane; and Vincent Lemort. "Empirical model of a variable speed vapor injection compressor for air source heat pump dynamic modeling." *International conference on compressors and their systems. 2015*.
[11] Bach, Christian K.; Braun, James E.; and Groll, Eckhard A., "A Virtual EXV Mass Flow Sensor for Applications With Two-Phase Flow Inlet Conditions" (2012). International Refrigeration and Air Conditioning Conference. Paper 2122.
[12] Park, Chasik, Honghyun Cho, Yongtaek Lee, and Yongchan Kim. "Mass flow characteristics and empirical modeling of R22 and R410A owing through electronic expansion valves." International Journal of Refrigeration 30, no. 8 (2007): 1401-1407.
[13] Christian JL Hermes, Robson O Piucco, Jader R Barbosa, and Claudio Melo. A study of frost growth and densication on at surfaces. Experimental Thermal and Fluid Science, 33(2):371-379, 2009.